UCRL-PROC-224273

LAWRENCE
LIVERMORE
NATIONAL
LABORATORY

Looking for anomalous dispersion in weakly ionized plasmas using X-ray laser interferometry

Joseph Nilsen, J. I. Castor, C. A. Iglesias, K. T. Cheng, J. Dunn, Walter R. Johnson, Jorge Filevich, J. Grava, M. Purvis, M. C. Marconi, J. J. Rocca

September 8, 2006

10th International Conference on X-ray Lasers
Berlin, Germany
August 20, 2006 through August 25, 2006

Disclaimer

Looking for anomalous dispersion in weakly ionized plasmas using X-ray laser interferometry

Joseph Nilsen, J. I. Castor, C. A. Iglesias, K. T. Cheng, and J. Dunn

Lawrence Livermore National Laboratory, Livermore, CA 94551

Walter R. Johnson

University of Notre Dame, Notre Dame, IN 46556

Jorge Filevich, J. Grava, M. Purvis, M. C. Marconi, J. J. Rocca

Colorado State University, Fort Collins, CO 80523

Summary. For decades the electron density of plasmas has been measured using optical interferometers. With the availability of good X-ray laser sources in the last decade interferometers have been extended into the wavelength range 14 – 72 nm, which has enabled researchers to probe even higher density plasmas. The data analysis assumes that the index of refraction is less than one and is due only to the free electrons in the plasmas. Recent interferometer experiments using Al plasmas observed an index of refraction greater than one at 14 nm and showed how the anomalous dispersion from bound electrons can dominate the free electron contribution to the index of refraction in many plasmas. Using our average-atom and atomic physics codes together with experimental data we searched for other plasmas that would have an index of refraction greater than one in an X-ray laser interferometer operating at 47 nm. We identified several promising candidates.

We present the calculations and the experimental confirmation that doubly ionized Ag, Sn, and C plasmas have an index of refraction greater than one at the 46.9 nm wavelength (26.44 eV) of the capillary discharge Ne-like Ar soft X-ray laser. These results show that bound electrons can dominate the index of refraction of numerous plasmas over a broad range of soft X-ray wavelengths.

1 Introduction

Since the early days of lasers, optical interferometers have been used to measure the electron density of plasmas [1] using the assumption that the index of refraction of the plasma is due only to the free electrons and is therefore less than one [1-2]. With this assumption the electron density of the plasma is directly proportional to the number of fringe shifts in the interferometer for conditions discussed in next section. Over the last decade many interferometers [3-8] have been built in the soft X-ray wavelength range of 14 to 72 nm (89 to 17 eV). The experiments done with these sources all assume that only the free electrons contribute to the index of refraction. In the future, interferometers will be built using the X-ray free electron lasers, which will extend lasers to even shorter wavelengths [9].

In the last three years interferometer experiments [4-6] of Al plasmas observed fringe lines bend in the opposite direction than was expected, indicating that the index of refraction was greater than one. Analysis of the experiments showed that the anomalous dispersion from the resonance lines and absorption edges of the bound electrons have a larger contribution to the index of refraction with the opposite sign as the free electrons [10-12]. Since the original analysis [10] of the experiments with Al plasmas we have developed a new tool [13] that enables us to calculate the index of refraction for any plasma at any wavelength. This tool is a modified version of the INFERNO average atom code [14] that has been used for many years to calculate the absorption coefficients for plasmas.

To understand how common the anomalous index of refraction effect is, we predict plasmas that have an index of refraction greater than one at the 46.9 nm (26.44 eV) wavelength of the Ne-like Ar X-ray laser [15] that is used at Colorado State University. This X-ray laser is a capillary discharge, table-top X-ray laser that has been used for more than a decade as a research tool. We present calculations of doubly-ionized Ag and Sn plasmas that predict an index of refraction greater than one and interferometer experiments that confirm our predictions. We analyze experiments done with C plasmas that show an index of refraction great than one.

2 Analysis of interferometer experiments

When the electron density is much less than the critical density, as is typical for laser produced plasmas, the traditional formula for the index of refraction of a plasma due only to free electrons is approximated as $n = 1 - (N_{elec} / 2N_{crit})$ where N_{elec} is the electron density of the plasma and N_{crit} is the plasma critical density. For a uniform plasma of length L the number of fringe shifts observed in an interferometer equals (1 – n) L / λ or (N_{elec} L) / (2 λ N_{crit}). When analyzing an experiment one counts how far the fringes have shifted compared with the reference fringes taken with no plasma and converts this into electron density. For the 46.9 nm Ne-like Ar X-ray laser the number of fringe shifts in the interferometer is (N_{elec} L) / (4.8 x 10^{18} cm^{-2}).

To understand the contribution of the bound electrons we look at the relationship between the absorption coefficient and the index of refraction. The total absorption coefficient $\alpha = N_{ion}\,\sigma = (4\,\pi\,\beta) / \lambda$ where N_{ion} is the ion density of the plasma, λ is the wavelength, σ is the absorption cross-section, and β is the imaginary part of the complex index of refraction n* defined by n* = 1 – δ – iβ. The real part of the index of refraction n = 1 – δ. The Henke tables [16] tabulate the dimensional-less optical constants f_2 and f_1 for neutral materials. These coefficients are related to δ and β by $\delta = f_1\, N_{ion} / (2\, N_{crit})$ and $\beta = f_2\, N_{ion} / (2\, N_{crit})$. From the total absorption cross-section σ we determine the optical constant f_2. We then derive the optical constant f_1 as a function of photon energy E using the Kramers-Kronig dispersion relation [17] by taking the principal value of the integral

$$f_1(E) = Z_{nuc} + \frac{2}{\pi}\, P.V. \int_0^{\infty} \frac{f_2(\varepsilon)\, \varepsilon\, d\varepsilon}{E^2 - \varepsilon^2}$$

where Z_{nuc} is the atomic number of the element. For neutral materials the oscillator sum rules insure that f_1 goes to zero at zero energy and Z_{nuc} at infinite energy. For an ionized plasma with average ionization Z* then f_1 = Z* at E = 0.

In the absence of any bound electrons f_1 is equivalent to the number of free electrons per ion. Taking the ratio of f_1 to the number of free electrons per ion gives the ratio of the measured electron density to the actual electron density. When the ratio is negative, the index of refraction is greater than one and the fringes bend the opposite direction than expected in the interferometer.

3 Finding Anomalous Dispersion in Tin and Silver Plasmas

To understand how general the bound electron contribution (anomalous dispersion) to the index of refraction is we looked for materials that would have an index of refraction greater than one at 26.44 eV. As a first step in this search we looked at the Henke tables to find neutral materials that have an absorption edge near 26 eV. Sn (Z=50) immediately stood out as a candidate with the N_4 $4d_{3/2}$ and N_5 $4d_{5/2}$ edges at 24.9 and 23.9 eV. [16] The next step was to see if the f_1 coefficient is negative at 26.44 eV since finding negative f_1 values for neutral materials is usually a good clue to find negative f_1 in plasma that are only a few times ionized. Since the lowest published value for f_1 in the Henke tables is at an energy of 30 eV we used the absorption coefficient f_2 , which has published values down to 10 eV, together with the Kramers-Kronig dispersion relation to extrapolate f_1 below 30 eV. Figure 1 shows our estimate of f_1 for various materials in the range Z = 42 to 51. Ag and Sn both have negative values of f_1 near 26 eV and look to be promising candidates. Since the reflectivity of grazing incidence optics depends on f_1 being positive an interesting experiment to verify the negative f_1 values would be to see if the X-ray laser does not reflect off the material at grazing incidence.

For neutral Sn the absorption coefficient from the N edge near 24 eV makes Sn too opaque at 26.44 eV to observe fringes in an interferometer. Singly ionized Sn is very opaque due to the strong 4d – 5p absorption line at 26.37 eV. For doubly ionized Sn the ionization potential has moved to 30.1 eV so the plasma now becomes much more transparent since the 26.44 eV Ar X-ray laser would not have enough energy to photo-ionize Sn^{2+}. From Ref. 18 we see that Sn^{2+} has 3 absorption lines at 26.72, 27.58, and 28.03 eV that have been measured experimentally. These are the $4d^{10}5s^2\ {}^1S_0 \rightarrow 4d^9 5s^2 5p^1\ {}^3P_1,\ {}^1P_1,\ {}^3D_1$ lines with absorption oscillator strengths of 0.071, 0.801, 0.067 respectively. The 26.44 eV X-ray laser is situated on the low energy side of these strong lines, so these lines will have a negative contribution to the f_1 value at this energy.

We estimate the index of refraction for the Sn plasma using the average atom code. We choose a Sn plasma with an ion density of 10^{20} cm^{-3} and a temperature of 4 eV because this gives Z* = 1.98, which means the plasma is, on average, doubly ionized. The solid line in Fig. 2 shows the optical constant f_1 versus photon energy calculated by the average atom code. This is compared with the more detailed calculation (dotted line) of f_1 for Sn^{+2} using a combination of the experimental data and theory as described in Ref. 19. We have excellent agreement between the two calculations in the region near 26 eV. At 26.44 eV the average atom code predicts f_1 = -10. Usually we would have to shift the energy scale of the average atom results but in this case the strong 4d -> 5p absorption line is within 0.1 eV of the experimentally measured value.

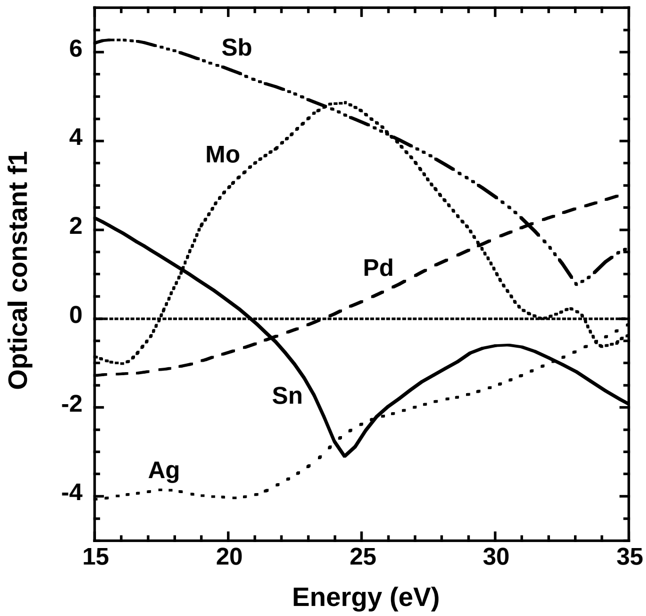

Fig. 1. Optical constant f_1 versus photon energy for cold neutral materials.

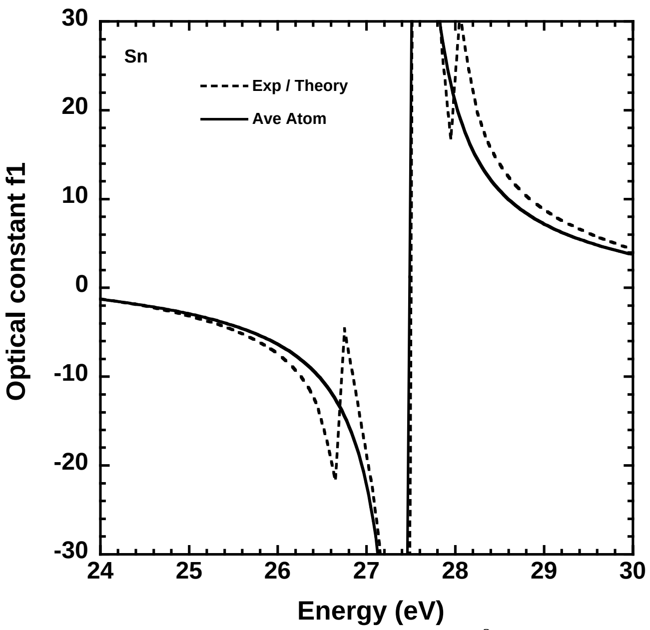

Fig. 2. Optical constant f_1 versus photon energy for Sn^{2+} calculated using experimental data and theory (dotted line) and using the average atom code (solid line).

We do not have experimental measurements of the Ag line positions as we did for Sn but based on calculations we expect that Ag^{2+} will have 4d – 4f and 4d – 6p lines in the 25 to 30 eV region that will result in a negative f_1 value at 26.44 eV. In addition the photo-ionization absorption edge for Ag^{2+} is at 35 eV which means absorption should be small at 26.44 eV. We did average atom calculations of a Ag plasma with ion density of 10^{20} cm^{-3} and a temperature of 4 eV which gives $Z^* = 2.08$. The structure is more complicated than Sn because of multiple strong lines but the average atom code predicts $f_1 = -7$ at 26.44 eV. It also predicts that f_1 will be less than zero from 21.8 to 27.8 eV. See Ref. 19 for more details.

4 Interferometer Experiments with Tin Plasmas

We used the interfereometer at Colorado State University with the 46.9 nm Ne-like Ar X-ray laser to search for Sn plasmas that had an index of refraction greater than one. The experiment is described in detail in Ref. 19. We determine the electron density by comparing how the fringes move compared to a set of reference fringes in the absence of any plasma. Since the change in the index of refraction is proportional to the electron density when only the free electrons contribute the fringes will always move to the right of the reference fringes for our setup. If the fringes move to the left of the reference fringes than the index of refraction is greater than one. From the above discussion it is clear that to observe this anomalous effect we need a plasma that is transparent to the probing X-rays and has a negative value of f_1 at 26.44 eV. In the experiments we create a hot Sn plasma with a laser and then wait for the plasma to cool down. Given the opaque nature of neutral and singly-ionized Sn at this energy we would expect to observe the anomalous effect when the plasma has cooled enough to be double-ionized and still transparent. This would be shortly before the plasma cools enough to become opaque.

Figure 3 shows interferograms of tin plasmas for semi-cylindrical grooved targets with a length of 0.1 cm and a diameter of 500 μm for the cylinder. At an early time of 4.5 ns after the plasma is created one observes large fringe shifts and the largest density near the center of the cylinder. These fringe shifts all move to the right, as expected. However at late time, 33 ns after plasma creation, one observes an opaque plasma near the surface of the semi-cylindrical groove. Near the center of the cylinder the fringes now shift to the left, indicating the index of refraction is greater than one. One reference fringe is shown as a solid line for comparison.

Similar results are observed for Ag plasmas where an index of refraction greater than one is observed at late time. More details of these experiments can be found in Ref. 19.

5 Experiments and Modeling of Carbon Plasmas

Recently we showed that the index of refraction of partially ionized C plasma was very complex for photon energies below 40 eV. [12] Using the Ar X-ray laser interferometer at 46.9 nm we observe an index of refraction great than one in C plasma, as shown in Fig. 4. At 5 ns after the creation of the C plasma one observes the highest density plasma in the center of the cylinder with the fringes moving to the right, as expected. However, near the surface of the target one observes fringes that move to the left of the reference fringes, indicating the index of refraction is great than one in this region. At 15 ns after plasma creation we observed most of the fringes moving to the left. More details can be found in Ref. 20. To understand this we first looked at the absorption characteristics of C.

For neutral C the ionization potential is at 11.26 eV. This L shell absorption edge moves to 24.38 eV for singly ionized C, which would make a plasma very opaque for the 26.44 eV X-ray laser. However the ionization potential for doubly ionized C moves to 47.89 eV, which makes the plasma quite transparent for the X-ray laser. Using the average atom code we then calculated the index of refraction for C^{2+}, C^{3+}, and C^{4+}, by using an ion density of 10^{20} cm^{-3} and plasma temperatures of 6, 10, and 30 eV to achieve $Z^* = 1.97$, 2.92, and 3.95, respectively. Since the main feature in the spectrum are the 2p – 3d lines in each of these ionization stages we shifted the energy scale of the average atom results to make sure that the photon energy of the main absorption feature agreed with the experimentally observed energies. This required a positive shift of 4.21, 1.95, and 12.3 eV for C^{2+}, C^{3+}, and C^{4+}, respectively. Figure 4 shows the optical constant f_1 divided by Z^* versus photon energy calculated by the average atom code. One observes that the f_1 is negative at 26.44 eV for the C^{2+} (solid line). As the 2p – 3d line shifts to higher energy for C^{3+}(dashed line), the ratio is 0.8 at 26.44 eV. As one continues to ionize the plasma to C^{4+} (dotted line), the ratio is near one over this entire energy range as the contribution from the bound electrons disappear. For C^{2+} we also calculated f_1 using experimental data and the detailed OPAL code and these both gave negative f_1 at 26.44 eV, in agreement with the average atom code.

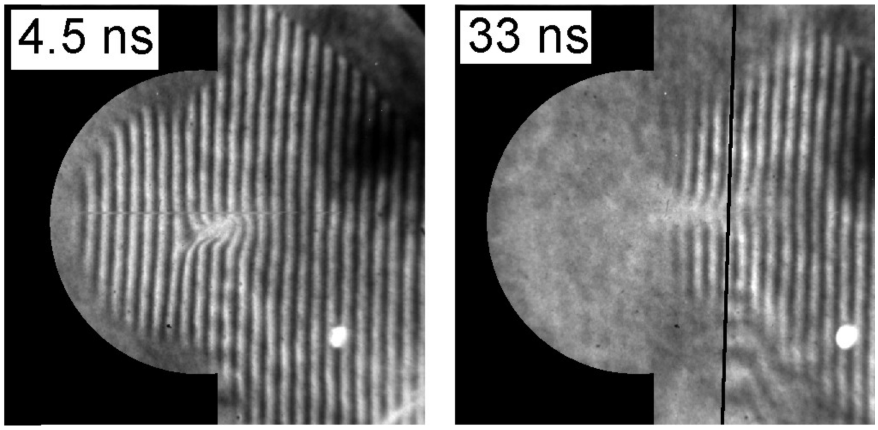

Fig. 3. Interferograms of Sn plasmas taken at two times during the evolution of the plasma. Time is relative to the creation of the plasma by the heating pulse. At early time (4.5 ns) the fringes all bend to the right but a late time (33 ns) some fringes bend to the left of the reference fringe (one shown by solid line) indicating an index of refraction greater than one.

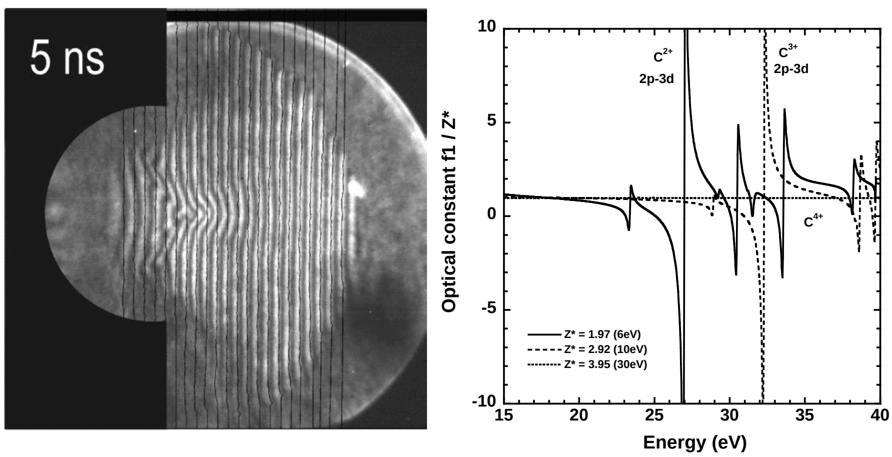

Fig. 4. Interferogram (left) of C plasma taken at 5 nsec after plasma generation. Fringes in the middle of the plasma are bending to the right however fringes near the target surface are bending to the left of the reference fringes (solid lines) indicating an index of refraction larger than one even at this early time. The right figure shows the optical constant f_1 divided by Z* versus energy for different ionizations of C plasmas showing f_1 is negative for C^{2+} at 26.44 eV. C^{2+} is solid line, C^{3+} is dashed line, and C^{4+} is dotted line near one over entire figure.

6 Conclusions

For decades the analysis of plasma diagnostics such as interferometers have relied on the approximation that the index of refraction in plasmas is due solely to the free electrons. This makes the index of refraction less than one and is an essential assumption used in determining the critical density surface for energy deposition in the plasma and for doing photon transport calculations. Recent X-ray laser interferometer measurements of Al plasmas at wavelengths of 14.7 and 13.9 nm observed anomalous results with the index of refraction being greater than one. The analysis of the Al plasmas show that the anomalous dispersion from both the resonance lines and absorption edges due to the bound electrons can have the dominant contribution to the index of refraction over the photon range from the optical up to 100 eV (12 nm) soft X-rays.

To understand how general this anomalous index of refraction effect is we searched for plasmas that should have an index of refraction greater than one at the 46.9 nm (26.44 eV) wavelength of the Ne-like Ar X-ray laser. We present calculations of doubly-ionized Ag, Sn, and C plasmas that predict an index of refraction greater than one and interferometer experiments that confirm our predictions.

During the next decade X-ray free electron lasers and other sources will be available to probe a wider variety of plasmas at higher densities and shorter wavelengths so it will be even more essential to understand the index of refraction in plasmas. X-ray laser interferometers may become a valuable tool to measure the index of refraction of plasmas in the future.

Acknowledgements

Work performed under the auspices of the US Department of Energy by the University of California Lawrence Livermore National Laboratory under Contract No. W-7405-Eng-48. This research was also sponsored by the National Nuclear Security Administration under the Stewardship Science Academic Alliances program through U. S. Department of Energy Research Grant # DE-FG52-06NA26152. The work of one author (WRJ) was supported in part by NSF Grant No. PHY-0139928.

References

1. G. J. Tallents, J. Phys. D. **17**, 721 (1984).
2. H. R. Griem, *Principles of Plasma Spectroscopy*, (Cambridge University Press, Cambridge, 1997) p. 9
3. L. B. Da Silva, T. W. Barbee, Jr., R. Cauble, P. Celliers, D. Ciarlo, S. Libby, R. A. London, D. Matthews, S. Mrowka, J. C. Moreno, D. Ress, J. E. Trebes, A. S. Wan, and F. Weber, Phys. Rev. Lett. **74**, 3991 (1995).
4. H. Tang, O. Guilbaud, G. Jamelot, D. Ros, A. Klisnick, D. Joyeux, D. Phalippou, M. Kado, M. Nishikino, M. Kishimoto, K. Sukegawa, M. Ishino, K. Nagashima, and H. Daido, Appl. Phys. B **78**, 975 (2004).
5. J. Filevich, J. J. Rocca, M. C. Marconi, S. Moon, J. Nilsen, J. H. Scofield, J. Dunn, R. F. Smith, R. Keenan, J. R. Hunter, and V. N. Shlyaptsev, Phys. Rev. Lett. **94**, 035005 (2005).
6. J. Filevich, J. J. Rocca, M. C. Marconi, S. Moon, J. Nilsen, J. H. Scofield, J. Dunn, R. F. Smith, R. Keenan, J. R. Hunter, and V. N. Shlyaptsev, J. Quant. Spectrosc. Radiat. Transfer **99**, 165 – 174 (2006).
7. J. Filevich, K. Kanizay, M. C. Marconi, J. L. A. Chilla, and J. J. Rocca, Opt. Lett **25**, 356 (2000).
8. D. Descamps, C. Lyngå, J. Norin, A. L'Hullier, C.-G. Wahlström, J.-F. Hergott, H. Merdji, P. Salières, M. Bellini, and T. W. Hänsch, Opt. Lett. **25**, 135 (2000).
9. A. Meseck, M. Abo-Bakr, D. Krämer, B. Kuske, and S. Reiche, Nucl. Inst. And Meth. A **528**, 577 (2004).
10. J. Nilsen and J. H. Scofield, Opt. Lett. **29**, 2677 (2004).
11. J. Nilsen and W. R. Johnson, Applied Optics **44**, 7295 – 7301 (2005).
12. J. Nilsen, W. R. Johnson, C. A. Iglesias, and J. H. Scofield, J. Quant. Spectrosc. Radiat. Transfer **99**, 425 – 438 (2006).
13. W. R. Johnson, C. Guet, and G. F. Bertsch, J. Quant. Spectrosc. Radiat. Transfer **99**, 327 – 340 (2006).
14. D. A. Liberman, JQSRT **27**, 335 (1982).
15. J. J. Rocca, V. Shlyaptsev, F. G. Tomasel, O. D. Cortázar, D. Hartshorn, and J. L. A. Chilla, Phys. Rev. Lett. **73**, 2192–2195 (1994).
16. B. L. Henke, E. M. Gullikson, and J. C. Davis, ADNDT **54**, 181 - 342 (1993).
17. L. D. Landau and E. M. Lifshitz, *Electrodynamics of Continuous Media*, (Pergamon, New York, 1984) pp. 280 - 283
18. P. Dunne, F. O'Reilly, G. O'Sullivan, and N. Murphy, J. Phys. B **32**, L597 (1999).
19. Jorge Filevich, M. Purvis, J. Grava, M. C. Marconi, J. J. Rocca, Joseph Nilsen, James Dunn, and Walter R. Johnson, Phys. Rev. E **74**, 016404 (2006).
20. J. Filevich, M. Purvis, J. Grava, M. C. Marconi, J. J. Rocca, J. Nilsen, J. Dunn, and W. R. Johnson, "Multiply ionized carbon plasmas with index of refraction greater than one," Laser and particle beams (in press from ECLIM 2006).